Potential Energy Surface of SCl_3^-

BettyCep D. Gailbreath,[†] Cynthia Ann Pommerening,[†] Steven M. Bachrach,*[,‡] and Lee S. Sunderlin*[,†]

Department of Chemistry and Biochemistry, Northern Illinois University, DeKalb Illinois 60115, and Department of Chemistry, Trinity University, San Antonio Texas 78212

Received: October 14, 1999; In Final Form: January 24, 2000

Sulfur trichloride anion is stable in the gas phase. Computational results at the G2 level indicate that SCl_3^- lies 99.0 kJ/mol below the dissociation products, dichlorosulfide and chloride anion, on a single-well potential energy surface. The anion has a T shape, with axial S−Cl bond lengths of 2.383 Å and an equatorial S−Cl bond length of 2.068 Å. Collision-induced dissociation results obtained using a flowing afterglow-tandem mass spectrometer give a $D_O(SCl_2-Cl^-)$ bond energy of 85 ± 8 kJ/mol.

Introduction

Nucleophilic substitution is a fundamental chemical reaction.[1] Most computational studies of substitution reactions have dealt with substitution at carbon atoms.[2] Recently more computational effort has been concentrated on reactions at heteroatoms such as nitrogen,[3] oxygen,[4] phosphorus,[5] and sulfur.[6,7] Substitution reactions at sulfur are of particular biological importance.[8] For example, the thiol−disulfide exchange reaction plays an important role in the folding of proteins. Disulfide bonds are critical in obtaining the proper lowest energy protein conformation; such bonds are often formed by a nucleophilic substitution reaction.[9] Thiol−disulfide exchange is also essential to the enzyme activities of flavin-containing dehydrogenases[10] such as lipoamide dehydrogenase, and glutathione reductase, which helps prevent the destruction of red blood cells. Several sulfide systems, particularly di- and trisulfides, have been analyzed and their nucleophilic substitution mechanisms determined theoretically.[6,7]

High-level calculations (including large basis sets and electron correlation) indicate that gas-phase substitution reactions of HS^- at organic sulfides (such as RSSR, where R can be H, CH_3, SH, or SCH_3) occur via an addition−elimination mechanism.[6,7] In these reactions, asymmetric transition states connect ion−dipole complexes with a stable intermediate (which is absent in many potential energy surfaces for substitution reactions).[11] The triple-well potential energy surface for this reaction is shown in Figure 1a. Studies on reactions of Cl^- and PH_2^- with $ClSCH_3$ and PH_2SCH_3, respectively, also indicate an addition−elimination mechanism.[12] While computationally analyzing the mechanism for the gas-phase nucleophilic substitution reaction of chloromethyl sulfide and chloride anion, a very stable intermediate (SI) was discovered. This intermediate, dichloromethyl sulfide anion, is 90.8 kJ/mol lower in energy than the reactants. As seen in Figure 1b, the SI is more stable than the ion−dipole complex, and the activation barrier between them is extremely small. The significant effect of substituting one organic substituent with a halogen suggested replacing the CH_3 on $ClSCH_3$ with another halogen and looking at its potential energy surface. This paper describes calculations and experiments on the identity substitution reaction of Cl^- with SCl_2.[13]

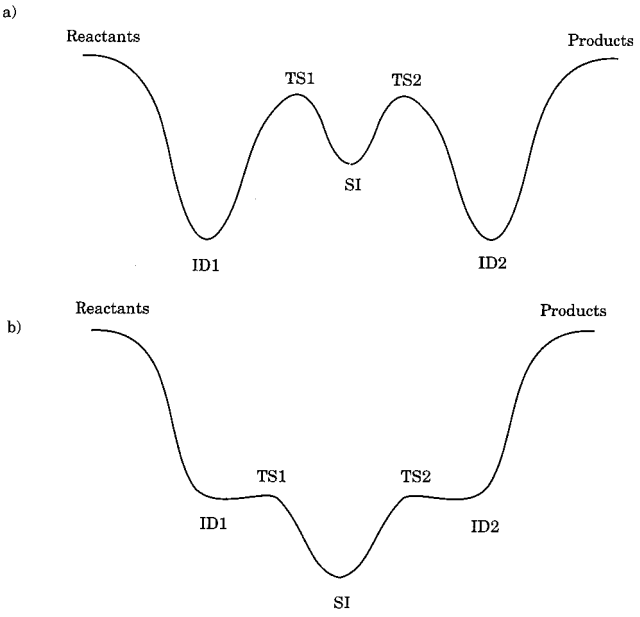

Figure 1. (a) Generalized B3LYP/aug-cc-pvDZ potential energy surface (PES) for di- and trisulfide nucleophilic substitution reactions. (b) B3LYP/aug-cc-pvDZ PES for the reaction of Cl^- with $ClSCH_3$.

The SCl_3^- anion is an example of hypervalent bonding.[14,15] The central sulfur atom has 10 electrons in its valence shell. Little is known about the gas-phase periodic trends and bond strengths in hypervalent systems. However, ACl_n-Cl^- bond strengths are available for $ACl_n = SiCl_4$,[16] PCl_3,[17] and ClCl,[15] and measurement of the SCl_2-Cl^- bond strength would allow the determination of the effect of the central atom on hypervalent bond strengths.

Computational Methods

Ab initio calculations were performed on the reactants and stable intermediate using GAUSSIAN 94 or 98.[18] The geometries of SCl_2, Cl^-, and SCl_3^- were optimized at the B3LYP level[19] using Dunning's correlation-consistent aug-cc-pVDZ basis set.[20] The relatively large cc-pVDZ basis set, which includes polarization functions, was augmented with diffuse functions to better account for the electron distribution in anions.

[†] Northern Illinois University.
[‡] Trinity University.

10.1021/jp993671w CCC: $19.00
Published on Web 03/09/2000

TABLE 1: Optimized Geometrical Parameters and Dissociation Energy[a]

	SCl_2		SCl_3^-			
level	S−Cl	Cl−S−Cl	$S-Cl_{(1)}$	$S-Cl_{(2)}$	$Cl_{(1)}-S-Cl_{(2)}$	*D*
B3LYP/aug-cc-pVDZ	2.072	103.65	2.109	2.406	96.75	115.2
B3LYP/aug-cc-pVTZ	2.050	103.86	2.086	2.392	96.62	107.6
B3PW91/aug-cc-pVTZ	2.031	103.83	2.063	2.359	95.42	107.4
G2	2.035	103.32	2.068	2.383	95.67	99.0

[a] All distances are in ångstroms, all angles are in degrees, and all energies are in kJ mol^{-1}.

Analytical frequencies were also calculated at the B3LYP/aug-cc-pVDZ level to obtain vibrational constants. The frequencies obtained were not scaled because the recommended B3LYP "low-frequency scaling factor" is 1.00.[21] Stable structures were confirmed by the existence of zero imaginary vibrational frequencies. Rotational constants were calculated from the optimized geometries. The lowest energy conformers for SCl_2 and SCl_3^- both had C_{2v} symmetry. A potential energy surface scan was also obtained at this level.

The B3LYP density functional method was used because of previous studies that dealt with nucleophilic substitution reactions that had sulfur as the central reactive atom. Bachrach and Mulhearn compared many different computational levels for the disulfur reactions, finding little variation among the energies or geometries using the Møller−Plesset (MP2, MP4), coupled cluster (CCSD), and DFT (B3LYP) methods.[6] Calculations at the present level of theory give EA(Cl) = 3.72 eV, in reasonable agreement with the experimental value of 3.61 eV.[22] In other studies of main group halides, Schaefer and co-workers found that the B3LYP method gave better agreement with the experimental dissociation energies for BrF,[23] PF,[24] and PF_3[24] than other density functional methods. There is also good agreement between experimental and B3LYP bond energies in PF_4^- and PF_6^-,[22,24] as well as $SF_n^{+/0/-}$ species.[25] On the other hand, the B3LYP bond energy for BrCl is 24 kJ/mol lower than the experimental value,[26] and agreement on electron affinities of PF_n systems is poor.[24,27] To further evaluate the efficacy of the B3LYP method, the dissociation energy of SCl_3^- was obtained by reoptimization of the geometries at B3LYP/aug-cc-pVTZ, B3PW91/aug-cc-pVTZ, and G2. The geometries and dissociation energies are listed in Table 1.

Experimental Section

The flowing afterglow tandem mass spectrometer used in these experiments consists of an ion source, a flow reactor, and a tandem mass spectrometer comprising a quadrupole mass filter, an octopole ion guide,[28] a second quadrupole mass filter, and a detector. This instrument has been described in detail previously;[29] a brief description follows.

The ion source used in these experiments is a dc discharge that typically operates at 1500 V with 2 mA of emission current. The ions for these experiments were produced by adding SCl_2 (Aldrich Chemical Tech Grade 80%, used as received) at the plasma source. Dissociative electron attachment to SCl_2 gives Cl^-, and attachment of the Cl^- to another molecule of SCl_2 gives SCl_3^-. The flow tube is a 92 cm × 7.3 cm i.d. stainless steel pipe with five neutral reagent inlets. The pressure in the flow tube is 0.4 Torr, as measured at the middle gas inlet by a capacitance manometer. The buffer gas flow velocity is 100 m/s, and ions undergo approximately 10^5 collisions with the buffer gas during their 10 ms residence in the flow tube. Since transfer of energy from low-frequency vibrational modes to translational energy during collisions is efficient, even SCl_3^- ions formed near the end of the flow tube are almost certainly equilibrated at room temperature. The buffer gas is typically 95% helium and 5% argon. Ions are sampled from the flow tube into the main chamber, which contains the tandem mass spectrometer. This chamber is differentially pumped to pressures sufficiently low that further collisions of the ions with the buffer gas are unlikely. The octopole passes through a gas cell that is filled with argon for collision-induced dissociation (CID) experiments.

Threshold Analysis. The threshold energy for a reaction is determined by modeling the intensity of product ions as a function of the reactant ion kinetic energy in the center-of-mass (CM) frame, E_{CM}. The translational energy zero of the reactant ion beam is measured using the octopole as a retarding field analyzer.[28,30] The first derivative of the beam intensity as a function of energy is approximately Gaussian, with a full-width at half-maximum of typically 1.0 eV. A small fraction of the ions can be translationally excited in excess of this distribution by the rf fields of the first quadrupole. This results in additional tailing at the lowest energies of the cross section data. The effect of this tailing is included in the overall uncertainty in the reported reaction thresholds. The laboratory energy E_{lab} is given by the octopole rod offset voltage measured with respect to the center of the Gaussian fit. Conversion to the CM frame is accomplished by use of $E_{CM} = E_{lab}m/(m + M)$, where m and M are the masses of the neutral and ionic reactants, respectively. This energy is corrected at low offset energies to account for truncation of the ion beam.[30]

Total cross sections for reaction, σ_{total}, are calculated using eq 1,[30] where I is the intensity of the reactant ion beam, I_0 is the intensity of the incoming ion beam ($I_0 = I + I_i$), and I_i are

$$I = I_0 \exp(-\sigma_{total} nl) \quad (1)$$

the intensities for each product ion. The number density of the neutral collision gas is n, and l is the effective collision cell length, 13 ± 2 cm.[29] Individual product cross sections σ_i are equal to $\sigma_{total}(I_i/I_i)$.

To derive CID threshold energies, the threshold region of the data is fitted to the model function given in eq 2, where $\sigma(E)$ is the cross section for formation of the product ion at

$$\sigma(E) = \sigma_0 \Sigma_i [g_i P_D(E,E_i)(E + E_i - E_T)^n/E] \quad (2)$$

center-of-mass energy E, E_T is the desired threshold energy, σ_o is a scaling factor, n is an adjustable parameter related to the shape of the cross section, P_D is the probability of an ion with a given amount of energy dissociating within the experimental window (ca. 30 μs), and i denotes rovibrational states having energy E_i and population g_i ($\Sigma g_i = 1$). P_D and the branching fractions for multiple dissociation pathways were calculated using the RRKM formalism. The CRUNCH program is used in the threshold analysis described above.[31]

The thermal motion of the collision gas (Doppler broadening) and the kinetic energy distribution of the reactant ion (which is approximated by a Gaussian function with the experimental fwhm) are also included in the fitting procedure. The effect of

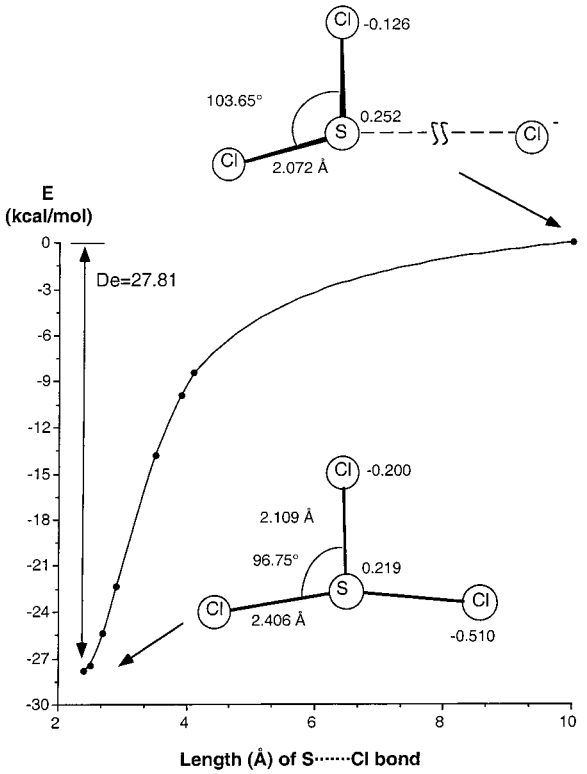

Figure 2. B3LYP/aug-cc-pvDZ energy surface for SCl_3^-. Geometrical parameters and natural population analysis charges are also shown.

secondary collisions is accounted for by linear extrapolation of data taken at several pressures to a zero pressure cross section.[32]

The derived reaction threshold can be affected by possible errors in the calculated frequencies, which determine the predicted internal energy of the reactant ions and the probability of dissociation, P_D. The possible effect was estimated by multiplying the derived reactant and product frequency sets by 0.8 and 1.2 and refitting the data with the scaled frequency sets. The resulting changes in the derived threshold were 0.01 eV or less, indicating that likely errors in the calculated frequencies have a negligible impact on the overall uncertainty of the measurements. The uncertainty associated with a factor of 3 change in the 30 μs time window for dissociation is also negligible (<0.001 eV). The uncertainty in the energy scale is 0.15 eV in the lab frame, or 0.034 eV in the CM frame. These uncertainties are combined with the standard deviation of the thresholds derived from different data sets to give the overall uncertainty in the reaction threshold.

Results

The computed structures for sulfur dichloride and the sulfur trichloride anion are shown in Figure 2. A single-well potential energy surface, also shown in Figure 2, is calculated for this reaction. Structures represented on this surface were obtained by fixing one S−Cl distance and optimizing all other geometric parameters. No ion−dipole complex or transition state was found. Local energy minimum structures, having no imaginary frequencies, were determined for SCl_2 and SCl_3^-. SCl_2 has a bent geometry, and SCl_3^- is roughly T-shaped. The latter geometry is consistent with both VSEPR theory and with the presence of a three-center−four-electron bond. It also agrees with expectations for a collinear Cl−S−Cl geometry for a nucleophilic substitution reaction. Addition of Cl^- to SCl_2 lengthens one of the original S−Cl bonds by only 0.037 Å,

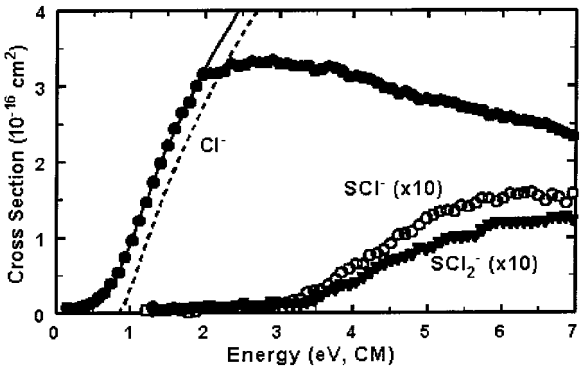

Figure 3. Appearance curves for collision-induced dissociation of SCl_3^- as a function of kinetic energy in the center-of-mass frame. The solid line is the model appearance curve calculated using eq 2 and convoluted as discussed in the text. The dashed line is the unconvoluted fit. The fitting parameters for this data set are $n = 1.38$ and $E_T = 0.86$ eV.

while the S−Cl bond opposite the incoming Cl^- is lengthened by 0.334 Å in the symmetric intermediate.

Natural population analysis (NPA) charges of the atoms in SCl_2 and SCl_3^- are given in Figure 2. These results are very consistent with the 3C−4E bonding model, which predicts charges of −0.5 on the terminal atoms of the hypervalent bond. Natural bond orbital (NBO) calculations give 1.8% d orbital character for the orbitals on the sulfur that are bonded to the two axial chlorine atoms. This is also more consistent with the 3C−4E model, rather than the expanded octet model.

CID Results. The data for collision-induced dissociation of SCl_3^- as a function of translational energy are shown in Figure 3. The reactions observed are given in eqs 3−5, where the neutral products are assumed on the grounds that other possible neutral products are at least 2.5 eV

$$SCl_3^- \rightarrow Cl + SCl_2^- \quad (3)$$

$$Cl_2 + SCl^- \quad (4)$$

$$SCl_2^- + Cl \quad (5)$$

higher in energy.[22] The two minor products have sufficiently small cross sections in the reaction threshold region that they can be ignored in the threshold fitting procedure. The optimized fitting parameters are $E_T = 0.88 \pm 0.07$ eV and $n = 1.4 \pm 0.2$. The threshold energy corresponds to a bond energy of 85 ± 8 kJ/mol after other sources of error are included. For comparison, the experimental bond energies in SCl_2 are roughly 3 times as strong: D(ClS−Cl) = 293 kJ/mol and D(S−Cl) = 240 kJ/mol.[22]

Reactions 3 and 5 involve competition between SCl_2 and Cl for the electron. The fact that reaction 3 has a lower threshold than reaction 5 is consistent with the electron affinity of chlorine, 3.61 eV, being higher than that of SCl_2. A quantitative analysis of this competition is in progress.[33] Reaction 4 is presumably a ligand coupling reaction, which should proceed without a barrier in excess of the endothermicity for this system.[34]

Bond Energies. The calculated dissociation energy at B3LYP/aug-cc-PVDZ is 115.2 kJ mol^{-1}. This value is in rather poor agreement with the experimental value, 85 ± 8 kJ mol^{-1}. Improving the basis set to aug-cc-pVTZ reduces the dissociation energy to 107.6 kJ mol^{-1} and essentially the same value is obtained using the B3PW91 functional. The geometries are only slightly affected by the basis set and functional type.

To obtain excellent agreement with experiment, calculation at the G2 level is required. Here, the dissociation energy is 99.0

TABLE 2: Periodic Trends in Bond Energies (kJ mol^{-1})

	SiX_4-X^-	PX_3-X^-	SX_2-X^-	X_2-X^-
X = F	251 ± 17[a]	168 ± 8.4[b]		
X = Cl	101 ± 8.4[a]	80 ± 7[c]	85 ± 8[d]	99 ± 5[e]

[a] Reference 16. [b] Larson, J. W.; McMahon, T. B. *J. Am. Chem. Soc.* **1983**, *105*, 2944−2950. [c] Reference 17. [d] This work. [e] Reference 15.

kJ mol^{-1}, within the combined error limits of the experiment and calculation. While the G2 geometries are very similar to the DFT geometries, clearly the DFT methods can provide only approximate dissociation energies. However, the most critical feature is the lack of any barrier or intermediate for this reaction, and all of the methods employed give this same qualitative potential energy surface.

Table 2 lists the measured bond strengths for ACl_n−Cl^- bond strengths for third row elements A. There is not a significant periodic trend in these bond strengths, indicating that the bond strength is reasonably independent of the central atom. However, substitution of fluorine for chlorine in these systems more than doubles the strength of the bond, indicating that the terminal atoms do affect the bond strength.

Potential Energy Surface for Substitution. Electronegative substituents stabilize the Cl(X)S−Cl^- ion-dipole complex by increasing the size of the dipole. Electronegative substituents also stabilize the intermediate by withdrawing electron density from the rest of the system. If the substituents are sufficiently electronegative, the barriers between the ion−dipole complexes and the stable intermediate disappear, leaving a single well. A more complete analysis of the effect of the nucleophile and leaving group on the mechanism for nucleophilic substitution at sulfur will be presented in a subsequent paper.[12]

Acknowledgment. Peter Armentrout and Kent Ervin are thanked for developing the improved version of the CRUNCH data analysis program. B.D.G. and C.A.P. thank the Graduate School of Northern Illinois University for financial assistance provided by Dissertation Completion Awards. The National Science Foundation provided partial support for this research.

References and Notes

(1) Lowry, T. H.; Richardson, K. S. *Mechanism and Theory in Organic Chemistry*, 3rd ed.; Harper & Row: Publishers: New York, 1987.
(2) Gronert, S. *J. Am. Chem. Soc.* **1991**, *113*, 6041−6048.
(3) Beak, P.; Li, J. *J. Am. Chem. Soc.* **1991**, *113*, 2796−2797. Bühl, M.; Schaefer, H. F., III. *J. Am. Chem. Soc.* **1993**, *115*, 9143−9147.
(4) Beak, P.; Loo, D. *J. Am. Chem. Soc.* **1986**, *108*, 3834−3835. Bachrach, S. M. *J. Org. Chem.* **1990**, *55*, 1016−1019.
(5) Li, J.; Beak, P. *J. Am. Chem. Soc.* **1992**, *114*, 9206−9207. Li, C. J.; Harpp, D. N. *Tetrahedron Lett.* **1993**, *34*, 903−906.
(6) Bachrach, S. M.; Mulhearn, D. C. *J. Phys. Chem.* **1996**, *100*, 3535−3540.
(7) Mulhearn, D. C.; Bachrach, S. M. *J. Am. Chem. Soc.* **1996**, *118*, 9415−9421.
(8) Mathews, C. K.; van Holde, K. E. *Biochemistry*; Benjamin/Cummings: Redwood City, CA, 1990.
(9) Liu, T.-Y. *The Proteins*; Academic Press: New York, 1977; pp 239−402.
(10) Williams, C. H., Jr. In *The Enzymes*; Boyer, P. D., Ed.; Academic Press: New York, 1976; Vol. 13, pp 89−173.
(11) Chabinyc, M. L.; Craig, S. L.; Regan, C. K.; Brauman, J. I. *Science* **1998**, *279*, 1882−1886.
(12) Bachrach, S. M.; Gailbreath, B. D. Manuscript in preparation.
(13) For a systematic study of the effects of varying the *nucleophilic* group, see: Hoz, S.; Basch, H.; Wolk, J. L.; Hoz, T.; Rozental, E. *J. Am. Chem. Soc.* **1999**, *121*, 7724−7725.
(14) *Chemistry of Hypervalent Compounds*; Akiba, K., Ed.; Wiley-VCH: New York, 1999.
(15) Nizzi, K. E.; Pommerening, C. A.; Sunderlin, L. S. *J. Phys. Chem. A* **1998**, *102*, 7674−7679.
(16) Larson, J. W.; McMahon, T. B. *J. Am. Chem. Soc.* **1985**, *107*, 766−773.
(17) Walker, B. W.; Sunderlin, L. S. Manuscript in preparation.
(18) (a) Gaussian-94: Frisch, M. J.; Trucks, G. W.; Schlegel. H. B.; Gill, P. M. W.; Johnson, B. G.; Robb, M. A.; Cheeseman, J. R.; Keith, T.; Petersson, G. A.; Montgomery, J. A.; Raghavachari, K.; Al-Laham, M. A.; Zakrzewski, V. G.; Ortiz, J. V.; Foresman, J. B.; Cioslowski, J.; Stefanov, B. B. Nanayakkara, A.; Challacombe, M.; Peng, C. Y.; Ayala, P. Y.; Chen, W.; Wong, M. W.; Andres, J. L.; Replogle, E. S.; Gomperts, R.; Martin, R. L.; Fox, D. L.; Binkley, J. S.; Defrees, D. J.; Baker, J.; Stewart, J. J. P.; Head-Gordon, M.; Gonzales, C.; Pople, J. A.; Gaussian, Inc.: Pittsburgh, PA, 1995. (b) Gaussian 98: Frisch, M. J.; Trucks, G. W.; Schlegel. H. B.; Scuseria, G. E.; Robb, M. A.; Cheeseman, J. R.; Zakrzewski, V. G.; Montgomery, J. A., Jr.; Stratmann, R. E.; Burant, J. C.; Dapprich, S.; Millam, J. M.; Daniels, A. D.; Kudin, K. N.; Strain, M. C.; Farkas, O.; Tomasi, J.; Barone, V.; Cossi, M.; Cammi, R.; Mennucci, B.; Pomelli, C.; Adamo, C.; Clifford, S.; Ochterski, J.; Petersson, G. A.; Ayala, P. Y.; Cui, Q.; Morokuma, K.; Malick, D. K.; Rabuck, A. D.;; Raghavachari, K.; Foresman, J. B.; Cioslowski, J.; Ortiz, J. V.; Baboul, A. G.; Stefanov, B. B.; Liu, G.; Liashenko, A.; Piskorz, P.; Komaromi, I.; Gomperts, R.; Martin, R. L.; Fox, D. L.; Keith, T.; Al-Laham, M. A.; Peng, C. Y.; Nanayakkara, A.; Gonzalez, C.; Challacombe, M.; Gill, P. M. W.; Johnson, B.; Chen, W.; Wong, M. W.; Andres, J. L.; Gonzalez, C.; Head-Gordon, M.; Replogle, E. S.; Pople, J. A.; Gaussian, Inc.: Pittsburgh, PA, 1998.
(19) (a) Becke, A. D. *J. Chem. Phys*. **1993**, *98*, 5648−5652. (b) Lee, C.; Yang, W.; Parr, W. G. *Phys. Rev. B* **1988**, *37*, 785.
(20) (a)Woon, D. E.; Dunning, T. H. *J. Chem. Phys*. **1993**, *98*, 1358−1371. (b) Kendall, R. A.; Dunning, T. H.; Harrison, K. R. *J. Chem. Phys*. **1992**, *96*, 6796−6806.
(21) Scott, A. P.; Radom, L. *J. Phys. Chem.* **1996**, *100*, 16502−16513.
(22) Mallard, W. G., Linstrom, P. J., Eds. *NIST Chemistry Webbook*; NIST Standard Reference Database Number 69, November 1998 release; National Institute of Standards and Technology: Gaithersburg MD 20899 (http://webbook.nist.gov).
(23) Pak, C.; Xie, Y.; Van Huis, T. J.; Schaefer, H. F., III. *J. Am. Chem. Soc.* **1998**, *120*, 11115−11121.
(24) Tschumper, G. S.; Fermann, J. T.; Schaefer, H. F., III. *J. Chem. Phys*. **1996**, *104*, 3676−3683.
(25) Bauschlicher, C. W.; Ricca, A. *J. Phys. Chem. A* **1998**, *102*, 4722−4727.
(26) Ignatyev, I. S.; Schaefer, H. F., III. *J. Am. Chem. Soc.* **1999**, *121*, 6904−6910.
(27) Gu, J.; Chen, K.; Xie, Y.; Schaefer, H. F., III; Morris, R. A.; Viggiano, A. A. *J. Chem. Phys*. **1998**, *108*, 1050−1054.
(28) Gerlich, D. *Adv. Chem. Phys.* **1992**, *82*, 1−176.
(29) Do, K.; Klein, T. P.; Pommerening, C. A.; Sunderlin, L. S. *J. Am. Soc. Mass Spectrom.* **1997**, *8*, 688−696.
(30) Ervin, K. M.; Loh, S. K.; Aristov, N.; Armentrout, P. B. *J. Phys. Chem.* **1983**, *87*, 3593−3596. Ervin, K. M.; Armentrout, P. B. *J. Chem. Phys.* **1985**, *83*, 166−189.
(31) (a) Rodgers, M. T.; Ervin, K. M.; Armentrout, P. B. *J. Chem. Phys.* **1997**, *106*, 4499−4508. (b) Rodgers, M. T.; Armentrout, P. B. *J. Chem. Phys.* **1998**, *109*, 1787−1800.
(32) (a) Loh, S. K.; Hales, D. A.; Lian, L.; Armentrout, P. B. *J. Chem. Phys.* **1989**, *90*, 5466−5485. (b) Schultz, R. H.; Crellin, K. C.; Armentrout, P. B. *J. Am. Chem. Soc.* **1991**, *113*, 8590−8601.
(33) Nizzi, K. E.; Gailbreath, B. D.; Pommerening, C. A.; Bachrach, S. M.; Sunderlin, L. S. Work in progress.
(34) Hoffmann, R.; Howell, J. M.; Muetterties, E. A. *J. Am. Chem. Soc.* **1972**, *94*, 3047−3058. Moc, J.; Dorigo, A. E.; Morokuma, K. *Chem. Phys. Lett.* **1993**, *204*, 65−72.